Dislocation reduction in GaN grown on porous TiN networks by metal-organic vapor-phase epitaxy

Y. Fu,[a] F. Yun, Y. T. Moon, Ü. Özgür, J. Q. Xie, X. F. Ni, N. Biyikli, and H. Morkoç
Department of Electrical and Computer Engineering, Virginia Commonwealth University, Richmond, Virginia 2284

Lin Zhou and David J. Smith
Center for Solid State Science and Department of Physics and Astronomy, Arizona State University, Tempe, Arizona 85287

C. K. Inoki and T. S. Kuan
Department of Physics, University at Albany, State University of New York (SUNY), Albany, New York 12222

(Received 12 August 2005; accepted 21 December 2005; published online 13 February 2006)

We report on the effectiveness of porous TiN nanonetworks on the reduction of threading dislocations (TDs) in GaN grown by metal-organic vapor-phase epitaxy (MOVPE). The porous TiN networks were formed by *in situ* annealing of thin-deposited Ti films deposited *ex situ* on GaN templates within the MOVPE growth chamber. Different annealing parameters in relation to surface porosity of TiN networks were investigated. Transmission electron micrographs indicated dislocation reduction by factors of up to 10 in GaN layers grown on the TiN nanonetwork, compared with a control sample. TiN prevented many dislocations present in the GaN templates from penetrating into the upper layer. Microscale epitaxial lateral overgrowth of GaN above TiN also contributed to TD reduction. The surface porosity of the TiN network had a strong impact on the efficiency of TD reduction. X-ray-diffraction and time-resolved photoluminescence measurements further confirmed the improved GaN quality. © *2006 American Institute of Physics*. [DOI: 10.1063/1.2170422]

I. INTRODUCTION

GaN and related nitrides have penetrated the marketplace in terms of short-wavelength light-emitting diodes and detectors, in spite of the fact that the electrical, optical, and structural properties of heteroepitaxial GaN are adversely affected by non-native substrates on which nitride materials are grown.[1] The resulting heteroepitaxial GaN has a high density of threading dislocations (TDs), typically 10^9-10^{10} cm^{-2} depending on the growth method, unless special measures are taken. The associated point defects cause leakage current, scatter-charged carriers, hamper radiative recombination efficiency, and cause device instabilities.[2] A large body of theoretical and experimental data point to many of the dislocations being electrically active, either due to nonfully coordinated bonding configuration around the dislocations and/or large local strain fields trapping charge carriers and impurities or point defects. The high TD density is increasingly detrimental to the performance of high-end devices with more sophisticated structures such as laser diodes, or electronic devices operating with high power density and frequency. Therefore, the reduction of defects in GaN epilayers is still an important issue. A TD density of 10^9 cm^{-2} or higher is typical for GaN grown on sapphire using AlN or GaN buffer layers due to large lattice and thermal mismatch.[3] Although SiC has smaller lattice mismatch to GaN, the TD density of GaN grown on SiC is comparable to that of GaN grown on sapphire, because the thermal mismatch is sufficiently large. Other possible substrates such as ZnO and $LiGaO_2$ produce inferior GaN material at this time. The lowest TD density (5×10^6 cm^{-2}) in GaN layer has been obtained in freestanding GaN templates grown by hydride vapor-phase epitaxy (HVPE).[4] Nevertheless, methods to reduce the defect concentration further during epitaxy of heterostructures even when freestanding GaN templates are used are imperative.

The epitaxial lateral overgrowth (ELO) technique with SiO_x- or SiN_x-patterned masks can significantly reduce TD density and enable device-quality GaN epilayers to the obtained.[5] The ELO process requires *ex situ* photolithographic step(s), where the frequency of the steps depends on how many times the process needs to be repeated for a given structure, which is both cumbersome and costly. To overcome this drawback, several groups have reported on the micro-ELO method using a discontinuous SiN_x network deposited *in situ* as a mask.[6,7] The SiN network is typically deposited on the GaN layer by simultaneously introducing silane and ammonia into a metal-organic vapor-phase epitaxy (MOVPE) growth chamber. The *in situ* SiN_x network growth reduces costs because all processes can be performed consecutively within the growth chamber.

Self-separation of HVPE-grown GaN templates from sapphire with the aid of a TiN interlayer was recently reported.[8] The relatively easy separation is attributed to voids formed at the GaN/TiN interface. It was also observed that some dislocations from the underlying GaN layer were

[a]Electronic mail: fuy@vcu.edu

 © 2006 American Institute of Physics

Downloaded 15 May 2006 to 128.172.168.211. Redistribution subject to AIP license or copyright, see http://jap.aip.org/jap/copyright.jsp

TABLE I. List of GaN templates and annealing time (for all Ti-covered GaN, annealing temperature is 1050 °C, and annealing gas ratios (NH_3:H_2) are 1:1 for T63 and 1:3 for other samples).

Sample	GaN template	Ti-thickness (nm)	Annealing time (min)	GaN grown on TiN (μm)	XRD FWHM (0002), ($10\bar{1}2$) (arc min)
Control-I	1 μm GaN/AlN	...	...	3.5	4.0,8.2
CVD481	buffer/SiC	10	10	3	4.4,5.7
CVD489		10	20	3	5.5,5.7
Control-II	0.7 μm	...	...	5	3.9,7.6
T63	GaN/GaN	20	30	13	4.4,4.6
T68	buffer/Sapphire	20	60	7.5	3.8,5.4

blocked from entering the upper layer by the TiN. A TD density of $(5-10)\times10^6$ cm^{-2} was achieved for GaN grown with TiN interlayer. However, the thickness of this HVPE-grown GaN reached 300 μm, and TD density on the order of 10^6 cm^{-2} was already available for HVPE-grown GaN template with similar thickness without any TiN interlayer.[4] In this particular case, due to the thickness of the layer, it is unclear to what extent which the TiN interlayer is responsible for the TD reduction. Thus, it would be useful to determine the efficiency of the TiN interlayer on TD reduction in thin GaN layers grown by MOVPE. Other potential advantages of applying a TiN interlayer in MOVPE process include TiN can be formed by *in situ* annealing of Ti films inside the MOVPE growth chamber without photolithographic processing, and Ti may be inactive during GaN growth and not act as undesired dopant. In the present paper, we report on the MOVPE growth and characterization of GaN layers on TiN porous networks. The TiN porous network was obtained by *in situ* annealing of thin Ti films deposited on thin GaN templates (~1 μm). Annealing parameters of TiN networks in MOVPE growth chamber have been investigated with respect to different surface porosities by scanning electron microscopy (SEM). Reduction of TD density by more than one order of magnitude was obtained for GaN grown on the TiN network, compared with control GaN. Transmission electron microscopy (TEM) images revealed that reduction of TD density resulted from dislocation blocking by the TiN layers and subsequent microscale ELO process of GaN on TiN. The improved GaN quality grown on TiN was confirmed by time-resolved photoluminescence (TRPL) and x-ray-diffraction (XRD) measurements.

II. EXPERIMENT

The TiN porous networks were formed by annealing thin Ti films deposited on GaN templates in mixed gases of ammonia and hydrogen. The GaN templates were grown on *c*-face sapphire and (0001) 6*H*-SiC substrates. The SiC wafers were annealed in H_2 at 1500 °C to eliminate polishing damage and to produce ordered atomic steps, followed by etching in molten KOH for 10 s to reduce surface defects, and dipping into a 1:10 HF acid solution for 1 min to remove the surface oxide. GaN growth was performed in a home-made vertical MOVPE chamber (radius of 5.5 in. and height of 15 in.) with ammonia (NH_3) and trimethylgallium (TMGa) as precursors for nitrogen and gallium, respectively. For all growth experiments, GaN epilayers were grown at 1030 °C at 76 torr reactor pressure. TMGa flows of 78 μmol/min were used, which would result in nominal planar growth rate of 1 μm/min. Ammonia flow rate was 0.31 mol/min and hydrogen was used as the carrier gas with flow rate of 0.4 mol/min. Two sets of GaN templates were chosen for this experiment: (1) 0.7-μm-thick GaN epilayers grown on a 25-nm-thick low-temperature (550 °C) GaN (LT-GaN) buffer on sapphire, and (2) 1-μm-thick GaN epilayers grown on a 100-nm-thick high-temperature (1100 °C) AlN (HT-AlN) buffer on SiC. The structure and growth conditions of the templates used in this experiment are listed in Table I.

Thin Ti films (10, 20, and 50 nm) were deposited on the (0001) surfaces of GaN templates at room temperature by electron-beam evaporation. The as-deposited Ti films were flat and featureless under SEM observation. These samples were then introduced into the MOVPE growth chamber, and annealed *in situ* in mixed H_2 and NH_3 at 1070 °C under a pressure of 200 Torr. Porous networks were formed on the sample surfaces under proper annealing conditions.

The final GaN layers were grown on the TiN networks by MOVPE at 1030 °C at 76 Torr. A V/III ratio of 4000 was employed with a TMGa flow rate of 78 μmol/min and NH_3 rate of 0.31 mol/min. 3-μm-thick GaN layers were grown on the TiN networks for samples CVD481 and CVD489, and 13 and 7.5 μm GaN layers were grown on TiN for samples T63 and T68, respectively. For comparison, two control samples were also grown on the same templates using identical growth conditions but without the TiN layer, as listed in Table I.

The surface of the TiN network was characterized using a JEOL JSM 6060 SEM operating at 10 kV. TEM was employed to investigate the effectiveness of the TiN network on TD reduction. The structural quality of the samples was evaluated by measuring both the symmetric (0002) and asymmetric ($10\bar{1}2$) XRD diffraction peaks using a Philips X'Pert MRD system equipped with a four-crystal Ge (220) monochromator. To study the radiative efficiency of GaN grown on TiN, TRPL spectroscopy was employed at room temperature using a 45 ps resolution Hamamatsu streak camera. The 3.82 eV excitation was incident at 45° to the surface normal, and the TRPL was collected normal to the surface.

Downloaded 15 May 2006 to 128.172.168.211. Redistribution subject to AIP license or copyright, see http://jap.aip.org/jap/copyright.jsp

III. RESULTS AND DISCUSSION

A. TiN formation

The surface porosity of the TiN networks was very sensitive to the annealing atmosphere, annealing time, and Ti thickness. After being annealed in pure NH_3 (flow rate of 0.3 mol/min) for 30 min, the surface of Ti/GaN remained flat with a few small pores. Based on the XRD analysis, this nitrided Ti shows diffraction peaks of (111)-oriented TiN,[8] suggesting the formation of a continuous TiN film on top of the GaN. High-resolution TEM indicated that this TiN layer was polycrystalline. In samples annealed in pure hydrogen for the same duration, we observed peeling off of most Ti films from the GaN, which may be due to the enhanced decomposition of GaN below Ti without ammonia. Provided a proper annealing time was used, porous TiN networks could be obtained in mixed NH_3 and H_2 with gas ratios ranging from 1:1 to 1:3.

We propose that formation of the porous TiN took place over three stages. First, the Ti film was turned into TiN by nitridation, as confirmed by XRD analysis and high-resolution TEM observations. Second, the continuous TiN layer got etched by hydrogen or decomposed at high annealing temperature. The etching or decomposition was likely to be initiated from boundaries of TiN polycrystals because defective regions are more active than others, which is consistent with the appearance of enclosed chains of small holes on the sample surface after several minutes of annealing. With continued annealing, these holes became larger, accompanied by the formation of new pores inside the grain boundaries. Finally, GaN partially decomposes in these pores and the porous TiN networks are formed.

Figures 1(a) and 1(b) show the surface morphologies of TiN networks for samples CVD481 and CVD489. Both samples have an identical template structure, i.e., 10 nm Ti/1 μm GaN/100 nm AlN buffer/SiC, and both went through the same annealing process except that CVD481 was annealed for 10 min and CVD489 was annealed for 20 min. The sizes of most pores on the surface of CVD481 are below 1 μm, and the pores are separated from each other by TiN. Both the density and sizes of the pores increase with annealing time, as shown by CVD489. Another set of samples, T63 and T68 with 20 nm Ti/0.7 μm GaN/GaN buffer/sapphire, exhibits similar porous TiN networks, as shown at higher magnification in Figs. 2(a) and 2(b). Detailed annealing parameters are again summarized in Table I. In T63 and T68, some GaN in large holes decomposed completely down to the sapphire substrate. The density of such holes is higher in T68 than T63. Connected trenches, which isolate the flattop GaN mesas, formed in T68.

While TiN networks could be obtained by depositing 10 and 20 nm of Ti, GaN templates coated with 50-nm-thick Ti were resilient to annealing. After 155 min of annealing, most of the surface remained flat except for a low density of large holes etched down to the substrate. This TiN layer provides a low density of overgrowth windows, making it difficult for the overgrown GaN surface to coalescence. For example, the

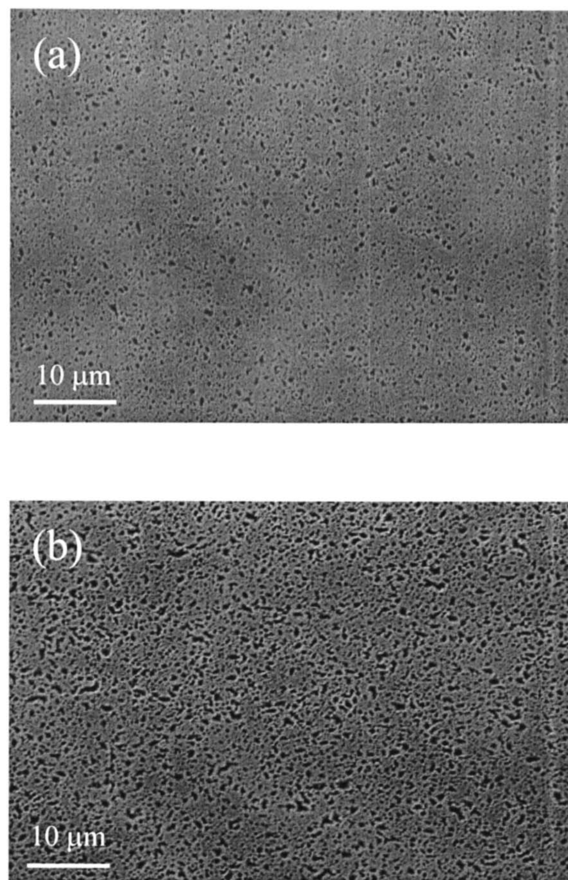

FIG. 1. SEM image of TiN networks on (a) CVD481, annealing for 10 min and (b) CVD489, annealing for 20 min.

GaN grown on this thick TiN for 6 h ($\sim$8 μm) still showed pinholes of more than 10 μm in diameter resulting from incomplete coalescence.

B. Characterization by TEM

For GaN growth at high temperature on continuous TiN layers obtained by annealing in pure ammonia, only sparse hexagonal GaN islands were observed. This result suggests poor wetting of the GaN nucleation layer on TiN, similar to GaN growth on SiO_x or SiN_x.[9] For the porous TiN network, GaN growth nucleates selectively at the pores by first filling the voids inside the pores, followed by appearance of small isolated GaN islands on the surface. With further growth, adjacent GaN islands expand and coalesce forming mesas as shown in Fig. 3. These mesas extend both vertically and laterally on TiN, leading eventually to full coalescence. It should be noted that the average distance between GaN islands is 2–3 μm while submicron distances were observed between many tiny pores in Figs. 1 and 2. This suggests that although high density of tiny pores formed on the TiN network, not all of them could act as effective nucleation sites. Similar phenomenon could be observed in GaN growth on TiN networks by HVPE (Ref. 8). In that case, higher density of small pores (average distance of less than 50 nm) was formed on TiN networks on 300 nm MOVPE-grown GaN as template, which was rather defective and easier to decompose. However, most GaN nucleation sites grown by HVPE

Downloaded 15 May 2006 to 128.172.168.211. Redistribution subject to AIP license or copyright, see http://jap.aip.org/jap/copyright.jsp

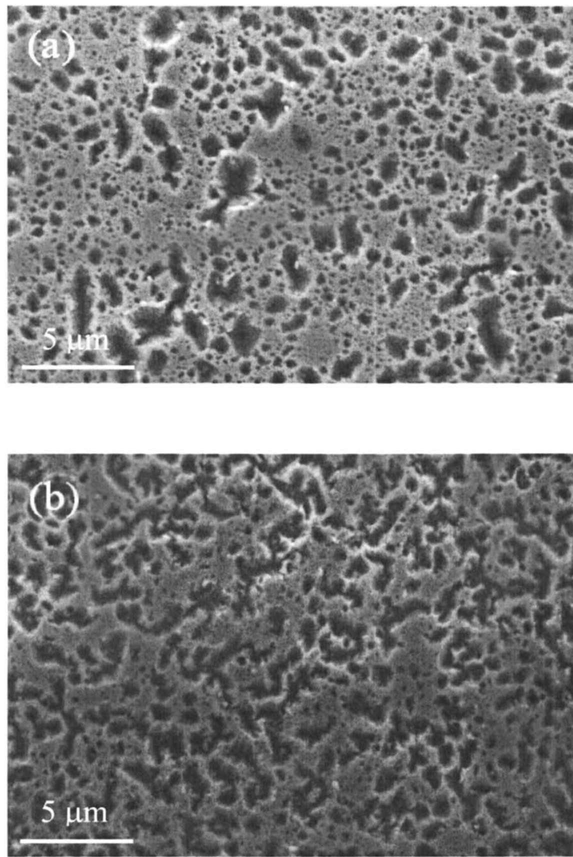

FIG. 2. SEM image of TiN networks on (a) T63, annealed for 30 min with $NH_3:H_2=1:1$ and (b) T68, annealed for 60 min with $NH_3:H_2=1:3$.

on TiN network were reported to have a distance of 5–10 μm. This might be attributed to mass transport from unstable tiny nucleation sites to larger nucleation sites.

Cross-sectional TEM observations were performed to investigate the mechanisms responsible for dislocation reduction. Conventional diffraction contrast images were obtained using two-beam conditions in order to identify the different types of TDs. Based on the visibility criteria $g \cdot b \neq 0$, screw and mixed type TDs are observable with $g=(0002)$, while edge and mixed type TDs are observable with $g=(11\bar{2}0)$. For given areas, images were obtained in the same region using both g vectors. Figures 4(a) and 4(b) compare the cross-

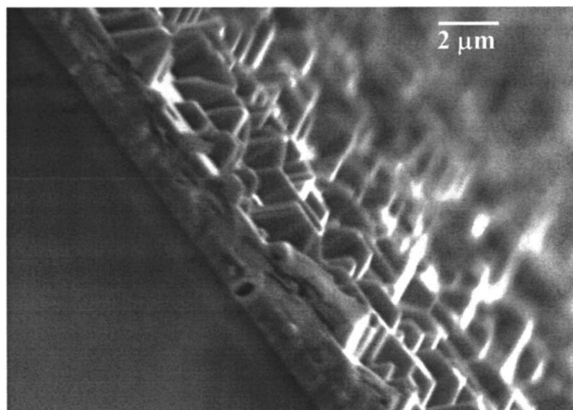

FIG. 3. SEM image showing GaN mesas initiated from pores on porous TiN network.

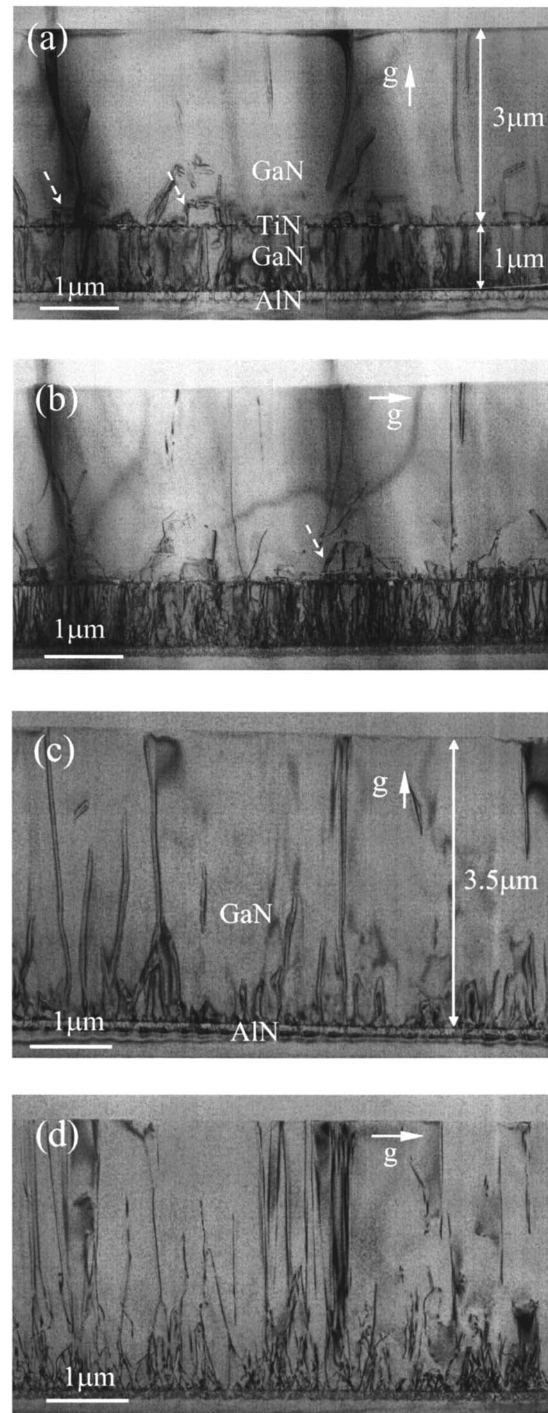

FIG. 4. Cross-sectional TEM images of CVD481 [(a) and (b)] and control GaN [(c) and (d)]. Images were taken under different conditions to show screw or mixed dislocations in (a) and (c) ($g=0002$), and edge or mixed dislocations in (b) and (d) ($g=11\bar{2}0$). Images of (a) and (b), and (c) and (d) come from almost the same areas, respectively.

sectional, bright-field TEM images of GaN grown on TiN network (CVD481) and the corresponding control sample. In the GaN template below the TiN network, a much higher TD density observed in Fig. 4(b) than that in Fig. 4(a), suggesting that the predominant TDs have edge-type component ($b=\langle 11\bar{2}0\rangle/3$), consistent with the data published earlier.[10] However, most TDs emanating from the GaN template are blocked from penetrating to the upper layer by the TiN and

Downloaded 15 May 2006 to 128.172.168.211. Redistribution subject to AIP license or copyright, see http://jap.aip.org/jap/copyright.jsp

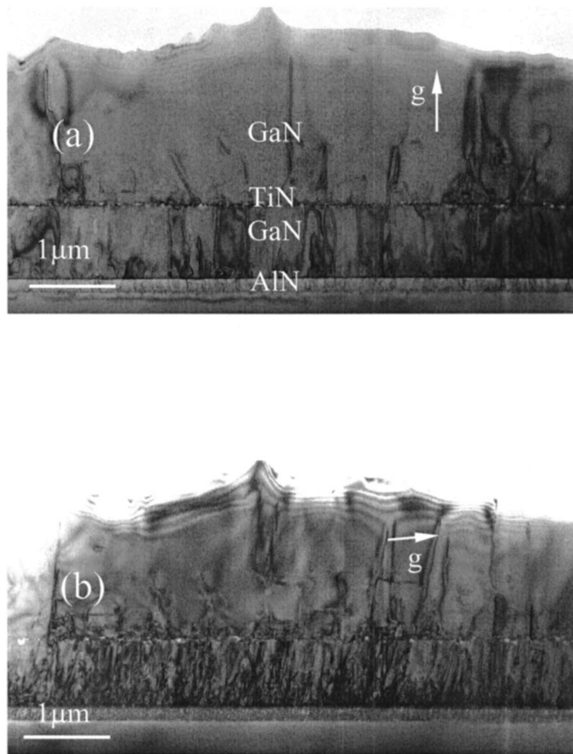

FIG. 5. Cross-sectional TEM images of CVD489 taken with (a) $g=0002$ to show screw or mixed dislocations and (b) $g=11\bar{2}0$ to show edge or mixed dislocations. Images of (a) and (b) come from almost the same areas.

the TDs above the GaN template are mainly mixed type ($\sim$70%). This indicates that the number of TD blocked by the TiN network is especially significant for edge-type dislocations. Although a small fraction of TDs pass through the network pores and enter the upper layer, many of them bend nearly 90° during the ELO process and extend laterally, finally annihilating each other by forming half-loops, as indicated by the dashed arrows in Figs. 4(a) and 4(b). It is noted that this dislocation interaction mechanism is observed to occur more effectively in Fig. 4(b) within the first 0.2 μm above the TiN. There are only a few TDs that extend further away vertically, and occasionally reach the top surface. Discontinuous planar voids with submicron size are observed above the TiN, due to ELO and poor wetting of GaN on TiN. These voids result in the elimination of the interface between TiN and the lateral overgrown GaN, which may help to release the interfacial stress and enhance the quality of coalesced fronts, which is consistent with the previous observations.[11] For comparison, Figs. 4(c) and 4(d) show the cross-sectional images of the control sample, which has no discernible dislocation reduction above the initial template.

As shown in Fig. 2, the TiN network in sample CVD489 has higher density and larger sizes of pores compared with CVD481 due to the longer annealing time. Figure 5 shows the TEM images of GaN grown on CVD489. In this sample, TDs were again effectively blocked by TiN and the ratio of edge and mixed-type dislocations was the same as that of sample CVD481. However, due to less TiN coverage on the template, a larger number of TDs penetrate into the TiN network and continue to extend vertically. This result suggests

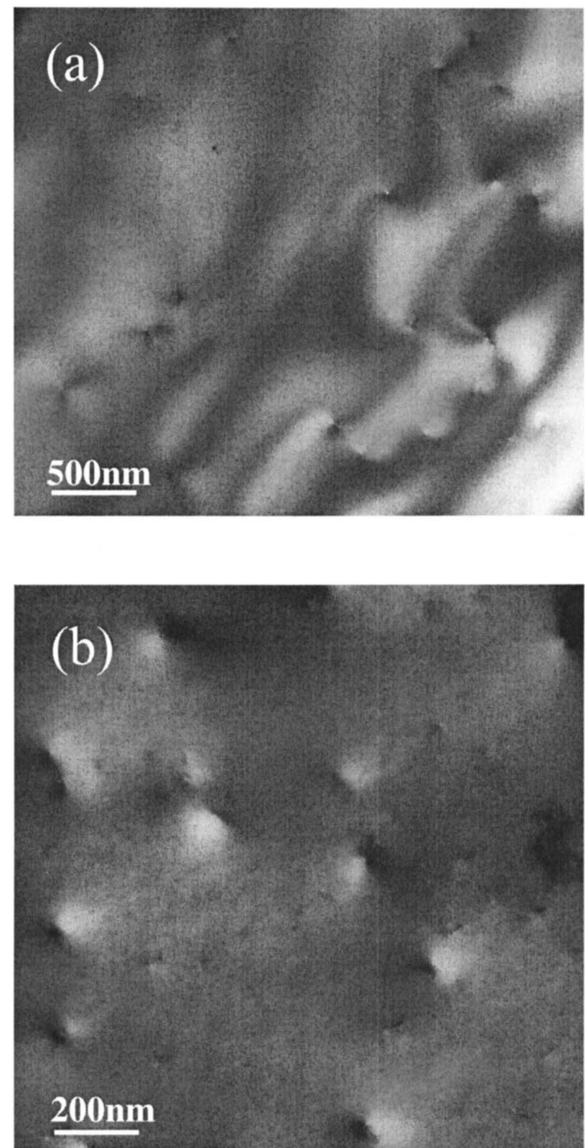

FIG. 6. Plan-view TEM image of (a) CVD 489 and (b) control GaN taken at [0001] zone axis showing edge-component dislocations.

that TiN networks from shorter annealing are likely to be more efficient for TDs reduction. On the other hand, a larger coverage of TiN (low density of nucleation sites) will render coalescence of GaN surface more difficult to achieve by MOVPE. In this vein, HVPE should be very suitable for GaN growth on TiN networks due to its high growth rate. In Ref. 8, the authors reported a 300-μm-thick GaN layer grown on TiN by HVPE with a low etching pits density of $(5-10)\times 10^{6}$ cm^{-2}. The authors of Ref. 8 reported the mechanism of dislocation reduction by TiN in HVPE growth to be very similar to than in MOVPE growth. However, they did not provide any data from a control sample which could have perhaps shed some light on clarify the efficacy of TiN networks on dislocation reduction in HVPE growth.

Plan-view images of CVD489 and the control GaN are shown in Fig. 6. Since edge-component dislocations are the major type of dislocations in these samples, reasonable estimation of the density could be made by directly counting the number of defects present in these images. The control GaN

Downloaded 15 May 2006 to 128.172.168.211. Redistribution subject to AIP license or copyright, see http://jap.aip.org/jap/copyright.jsp

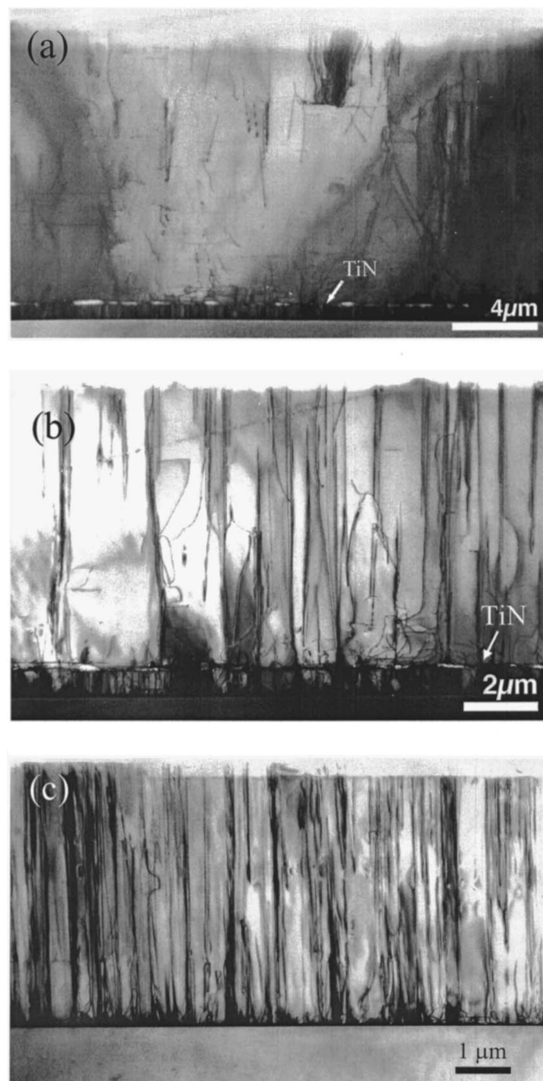

FIG. 7. Bright-field cross-sectional TEM image of (a) T63 and (b) T68 and (c) control GaN, taken with multibeam condition to show all dislocations present in the layers.

grown without using TiN shows a high density of edge dislocation arrays ($\sim 3\times10^{9}$ cm^{-2}), and a much lower density of end-on mixed dislocations ($\sim 8\times10^{8}$ cm^{-2}). The plan-view image of CVD489, on the other hand, shows significantly lower ($\sim 10\times$) density of edge dislocations ($\sim 2\times10^{8}$ cm^{-2}). This comparison clearly indicates the effectiveness of TiN in reducing the edge dislocation density. However, the densities of mixed TDs of CVD489 are only two times smaller (3×10^{8} cm^{-2}) than that of the control sample, which may result from two causes. First, the number of mixed TDs is already small (about 20% of the total dislocations) in the GaN template below TiN. Therefore, the impact of TiN in reducing the density of the mixed dislocations is smaller. Second, in the control sample, the density of mixed TDs drops with increasing thickness through dislocation reaction such as the fusion mechanism.[12] Moreover, the probability of mixed TDs reacting with each other is lower in CVD489 because the TD density is already reduced by the TiN, as shown in Fig. 5(a). Furthermore, we cannot rule out the possibility of dislocation generation at the coalescence fronts of GaN mesas on TiN, which may increase the mixed TD density. We observed similar dislocation reduction efficiency of the TiN network on the GaN templates on SiC using GaN buffers.

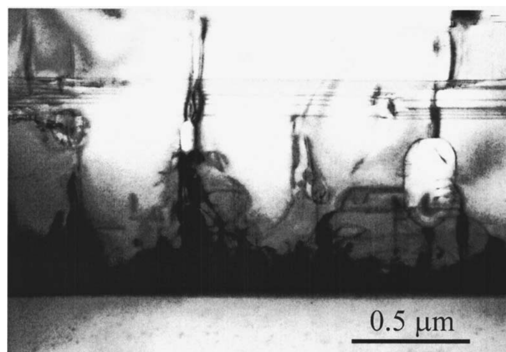

FIG. 8. Consolidation of dislocations at subsurface voids below TiN network. The stacking faults resulted from horizontal movements of partial dislocations.

Figure 7 shows the TEM images of GaN samples grown on T63 and T68, and the control sample II. The template for this set of samples is 0.7 μm GaN/LT-GaN buffer/sapphire with predominantly edge-type TDs, similar to the GaN template grown with HT-AlN buffer on SiC. Figure 7(a) shows that both the windows, and TiN between the windows, have an average size of ~ 1 μm for T63, so that the TiN has a surface coverage of $\sim 50\%$. The size of the windows in T68 increases to 3–4 μm with reduced TiN coverage.

Using plan-view images for the control sample grown without the TiN layer, we found the dislocations were predominantly edge type ($\sim 1.5\times10^{9}$ cm^{-2}) with less than 10% screw dislocations ($\sim 1.3\times10^{8}$ cm^{-2}). In T63 we saw a significant ($\sim 10\times$) reduction due to TiN of edge dislocations ($\sim 1.6\times10^{8}$ cm^{-2}), but the screw dislocations remain at the same low level ($\sim 0.7\times10^{8}$ cm^{-2}). The edge dislocations in T68 are reduced even more (by a factor of ($\sim 15-\sim 0.9$) $\times10^{8}$ cm^{-2}), while the density of screw dislocations remain more or less the same ($\sim 1.4\times10^{8}$ cm^{-2}).[13] It is noted that these dislocation density values are measured from the very top GaN layer. Since the dislocation density tends to decrease with layer thickness, and both T63 (13 μm) and T68 (7.5 μm) are thicker than the control sample (5 μm) (Table I), the amount of dislocation reduction due to the TiN layer would be slightly smaller than these measured values. We grew such thick GaN layers on the TiN/GaN/sapphire templates for the purpose of obtaining nearly coalescent top surfaces. However, on the TiN/GaN/SiC templates, a flattop surface was obtained for a 3 μm overgrown GaN layer. This difference may be attributed to different lateral growth rates of GaN on different TiN/GaN/substrate templates, and requires further study.

For GaN grown on TiN networks with longer annealing times, Fig. 8 shows that voids exist not only above the TiN but also below it. These voids below the TiN layer have a round shape with sizes less than ~ 0.3 μm. It was observed that many adjacent TDs were attracted by the voids, which consolidated them into a single TD which extended vertically. We believe that these voids evolve from the large hole

Downloaded 15 May 2006 to 128.172.168.211. Redistribution subject to AIP license or copyright, see http://jap.aip.org/jap/copyright.jsp

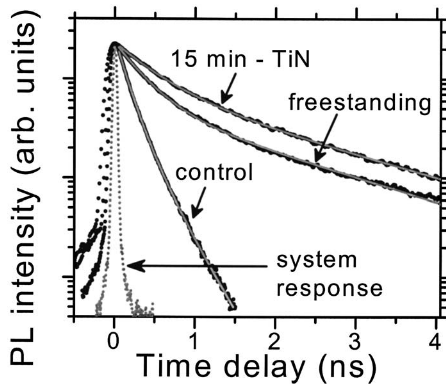

FIG. 9. Normalized TRPL spectra for a 6.8 μm GaN grown on TiN network, the control sample, and a freestanding GaN grown by HVPE. The solid lines are biexponential fits to the data.

inside GaN which completely decomposed during annealing. GaN growth in these large holes was initiated and then proceeded laterally from the sidewalls, which induced bending or inclination of TDs towards the centers of the holes. A similar growth process was reported by Nitta *et al.*[14] In some regions, due to the rapid lateral extension of GaN on the TiN layer, the holes were buried before refilling so that voids were formed.

IV. XRD AND TRPL MEASUREMENTS

High-resolution x-ray rocking curves (ω scan) show that the GaN layers grown on the TiN networks have improved crystalline quality as measured by the full width at half maximum (FWHM) of asymmetric $(10\bar{1}2)$ diffraction peaks, as shown in Table I. This result is consistent with the $\sim 10 \times$ reduction of TD density deduced from TEM observations, since the FWHM of the $(10\bar{1}2)$ diffraction peak is sensitive to the both screw component and edge component TDs, whereas (0002) diffraction is only sensitive to screw component TDs. The slightly higher (0002) FWHM values of CVD481 and CVD489 than that of the control sample can be explained by the comparable density of screw TDs in these samples. Similar explanation accounts for higher XRD (0002) FWHM value of T63 than that of its control GaN.

Preliminary electrical measurements were made on these GaN layers grown on TiN networks. The electron concentration and mobility of GaN grown with and without TiN network are comparable. Experiments to improve the electrical properties of GaN grown on TiN are in progress.

Figure 9 shows the TRPL results for a 6.8 μm GaN grown on TiN network (using the same template on sapphire as listed in Table I, but with 10 nm Ti and 15 min annealing), the control sample, and a HVPE-grown 200 μm freestanding GaN. The GaN grown on the TiN network exhibits decay times of $(\tau_1, \tau_2) = (0.47 \text{ ns}, 1.86 \text{ ns})$, which are significantly longer than those of the control sample, and are comparable to those of the freestanding HVPE GaN template. The longer carrier lifetimes indicate that radiative efficiency of GaN can be greatly improved by using TiN network. The detailed TRPL investigation of GaN grown on TiN networks has been reported elsewhere.[15]

V. SUMMARY

In summary, we have demonstrated that the density of TDs in GaN, particularly edge/mixed-type TDs, can be efficiently reduced by overgrowth on a porous TiN network obtained by *in situ* annealing in the MOVPE growth chamber. Transmission electron micrographs show that the TiN layer is effective in blocking the extension of most TDs from the underlying template. The microscale lateral overgrowth of GaN above TiN also contributes to TD reduction. By varying the TiN and subsequent annealing parameters, an order of magnitude reduction in the TD density was obtained. XRD and TRPL measurements further confirmed the improved GaN quality resulting from the reduced TD density.

ACKNOWLEDGMENTS

The work at Virginia Commonwealth University and University at Albany, State University of New York, is funded by ONR as part of a Defense University Research Initiative on Nanotechnology (DURINT) program, monitored by Dr. C. E. C. Wood, and the work at ASU was partially supported by the Office of Naval Research under Grant No. N-00014-04-1-0020. The authors thank Professor R. M. Feenstra (Carnegie Mellon University), Professor A. A. Baski (Virginia Commonwealth University), and Professor D. Johnstone (Virginia Commonwealth University) for helpful discussions, and the use of TEM facilities at Arizona State University is acknowledged.

[1] H. Morkoç, *Nitride Semiconductors and Devices*, 2nd ed. (Springer, Berlin, in press).
[2] Michael A. Reshchikov and Hadis Morkoç, J. Appl. Phys. **97**, 103407 (2005).
[3] P. Visconti, M. A. Reshchikov, K. M. Jones, D. F. Wang, R. Cingolani, H. Morkoç, R. J. Molnar, and D. J. Smith, J. Vac. Sci. Technol. B **19**, 1328 (2001).
[4] P. Visconti, K. M. Jones, M. A. Reshchikov, F. Yun, R. Cingolani, H. Morkoç, S. S. Park, and K. Y. Lee, Appl. Phys. Lett. **77**, 3743 (2000).
[5] P. Gibart, B. Beaumont, and P. Vennegues, in *Handbook on Materials and Devices and Devices*, edited by P. Ruterana, M. Albrecht, and J. Neugebauer (Wiley-VCH, Weinheim, 2003), Chap. 2.
[6] A. Sagar, R. M. Feenstra, C. K. Inoki, T. S. Kuan, Y. Fu, Y. T. Moon, F. Yun, and H. Morkoç, *Proceedings of the International Workshop on Nitride Semiconductors* [Phys. Status Solidi A 202, 772 (2005)].
[7] S. Sakai, T. Wang, Y. Morishima, and Y. Naoi, J. Cryst. Growth **221**, 334 (2000).
[8] A. Usui, T. Ichihashi, K. Kobayashi, H. Sunakawa, Y. Oshima, T. Eri, and M. Shibata, Phys. Status Solidi A **194**, 572 (2002); Y. Oshima, T. Eri, M. Shibata, H. Sunakawa, and A. Usui, *ibid.* **194**, 554 (2002).
[9] T. S. Zheleva, O.-H. Nam, M. D. Bremser, and R. F. Davis, Appl. Phys. Lett. **71**, 2472 (1997).
[10] W. Qian, M. Skowronski, M. De Graef, K. Doverspike, L. B. Rowland, and D. K. Gaskill, Appl. Phys. Lett. **66**, 1252 (1995).
[11] M. H. Kim, Y. Choi, J. Yi, M. Yang, J. Jeon, S. Khym, and S.-J. Leem, Appl. Phys. Lett. **79**, 1619 (2001).
[12] C. J. Lu, L. A. Bendersky, H. Lu, and W. J. Schaff, Appl. Phys. Lett. **83**, 2817 (2003).
[13] Y. Fu, Y. T. Moon, F. Yun, Ü. Özgür, J. Q. Xie, S. Doğan, and H. Morkoç, Appl. Phys. Lett. **86**, 043108 (2005).
[14] S. Nitta, T. Kashima, M. Kariya, Y. Yukawa, S. Yamaguchi, H. Amano, and I. Akasaki, MRS Internet J. Nitride Semicond. Res. **5S1**, W2.8 (2000).
[15] Ü. Özgür, Y. Fu, Y. T. Moon, F. Yun, H. Morkoç, H. O. Everitt, S. S. Park, and K. Y. Lee, Appl. Phys. Lett. **86**, 232106 (2005).

Downloaded 15 May 2006 to 128.172.168.211. Redistribution subject to AIP license or copyright, see http://jap.aip.org/jap/copyright.jsp